MJFAS
Malaysian Journal of Fundamental and Applied Sciences

Ibrahim *et al.* | Malaysian Journal of Fundamental and Applied Sciences, Vol. 21 (2025) 2738–2746

RESEARCH ARTICLE

Structure of Intermolecular Drug-Polymer Interactions: Ascorbic Acid–PVP K30 Complex

Nur Balqish Ezlyn Ibrahim[a], Nur Shasha Erina Sharief Halim[b], Faizani Mohd-Noor[b,*], Siti Maisarah Aziz[a,*]

[a]UniSZA Science and Medicine Foundation Centre, Universiti Sultan Zainal Abidin, Gong Badak Campus, 21300 Kuala Nerus. Terengganu, Malaysia; [b]Department of Physics, Faculty of Science, Universiti Teknologi Malaysia, 81310 UTM Johor Bahru, Johor, Malaysia

Abstract Ascorbic acid (AA) is widely used in pharmaceuticals and food industries, predominantly exists in a crystalline form due to its strong intramolecular hydrogen bonding and high lattice energy. This research explores the structural and intermolecular interactions of AA in a co-amorphous system with polyvinylpyrrolidone K30 (PVP K30), prepared by melt-quenching. The findings reveal that various hydrogen bonding between the hydroxyl groups of AA and the carbonyl groups of PVP K30 plays a key role in forming the amorphous phase. The broadening and shifting of vibrational peaks in FTIR spectra suggest intermolecular interactions, supported by DFT calculations that show reduced HOMO-LUMO energy gaps and enhanced dipole moments in the complex system. FTIR suggests molecular-level interactions promoting amorphization consistent X-ray diffraction (XRD) analysis that confirm the presence of some degree of amorphicity based on peak broadening. This highlights the complex interplay between local molecular interactions and long-range structural organization. Despite the limitations, the results indicate that PVP K30 has the potential to reduce the crystallinity of ascorbic acid and stabilize the amorphous phase, yet not completely. These findings provide insight into the challenges of achieving full amorphization and suggest further optimization in polymer selection and preparation techniques for improved stability.

Keywords: FTIR spectroscopy, DFT calculation, amorphous, crystalline, ascorbic acid, PVP K30, melt-quenching.

***For correspondence:**
smaisarahaziz@unisza.edu.my

Received: 17 April 2025
Accepted: 4 August 2025

Introduction

Ascorbic acid (AA) is well-known for its antioxidant properties, and it is widely utilized in the pharmaceutical and food industries.[1] Despite its extensive use, AA predominantly exists in its crystalline form due to its strong intramolecular hydrogen bonding and high lattice energy, which make its crystalline form thermodynamically more favourable.[2-3] Additionally, ascorbic acid is highly sensitive to environmental conditions such as heat, oxygen, and light, resulting in rapid degradation that poses significant challenges to its stability during storage and processing.[4-5] These inherent limitations in the crystalline AA and its use makes it a relevant subject for research and potential improvements, to study the amorphous nature of materials, as the transition to the amorphous state could potentially address these issues.

Preparing drugs in their amorphous form presents significant challenges due to their metastable nature, which makes pure amorphous compounds prone to crystallization.[6-7] This issue is particularly prominent in ascorbic acid, due to its low glass-forming ability as it possesses a very unstable amorphous phase and tendency to crystallize at ambient temperatures.[8] Polymer-based amorphous system formulations have consistently demonstrated efficacy in improving the physical stability of the amorphous form. By interacting at the molecular level, the added component forms intermolecular interactions such

as hydrogen bonding, leading to a structure that is unable to find a new crystalline order.[9] To stabilize AA in its amorphous form, polymers like polyvinylpyrrolidone K30 (PVP K30) are added as this polymer commonly used in the amorphous pharmaceutical formulation.[10-13] PVP K30 has the ability to interact with ascorbic acid at the molecular level, potentially forming intermolecular bonds that inhibit crystallization. These interactions can reduce molecular mobility and increase the energy barrier for phase transitions, thus promoting the formation and stabilization of the amorphous phase.[11-12,14] Similarly, hydrogen bonding with PVP K30 enabled the successful amorphization of metronidazole, which played a key role in preventing crystallization.[15]

The amorphous structure, characterized by higher internal energy, increased Gibbs free energy, and greater thermodynamic instability compared to its crystalline form, influences the material's phase behavior, thermal stability, and molecular dynamics.[16] The challenge in amorphous material research lies in unraveling the precise mechanisms governing phase transitions and understanding the role of intermolecular forces in maintaining stability. The lack of long-range order amorphous systems further complicates the characterization of their structural and dynamic properties. To address these challenges, a complementary approach is required, employing experimental techniques like X-ray diffraction (XRD) and Fourier-transform infrared (FTIR) spectroscopy with theoretical modelling, density functional theory (DFT). This approach not only offers deeper insights into the physical principles governing amorphous systems but also highlights the structural and dynamic interplay between AA and PVP K30. Unlike previous studies, this work uniquely explores the AA–PVP K30 system formed via the melt-quenching technique, providing valuable understanding of the structural and molecular dynamics in co-amorphous formulations. By analysing changes in vibrational spectra and electronic structure, this research further elucidates the underlying stabilization mechanisms within the co-amorphous system.

Materials and Methods

Amorphous samples were prepared using ascorbic acid (AA) purchased from Sigma-Aldrich and PVP K30 polymer from Inno Lab Engineering Sdn Bhd. Preparation of the samples was done by using the melt-quenching technique via the co-amorphous route. Lab-grade crystalline powders of pure substances are weighted according to the correct nominal composition. The nominal compositions utilized in this study were $x(C_6H_8O_6)$ - $(100\text{-}x)(C_8H_9NO)_n$, where x = 0, 20, 40, 60, 80 and 100 mol %. The mixture powder was melted in an alumina crucible at a melting temperature (190^{o}C) for 20 minutes. The melt was then quickly quenched by pouring the melt on the metal plate at 25^{o}C and powdered for analysis.

Vibrational Analysis

Intermolecular interaction between compounds in a co-amorphous system was evaluated using attenuated total internal reflection (ATR) A Perkin Elmer System 2000 FT-IR spectrometer. The samples, approximately 0.02 mg in powder form, were thoroughly mixed and ground with 2 mg of potassium bromide (KBr) using an agate mortar. The resulting mixture was transferred into a 13 mm diameter barrel. Transparent disc pellets were then formed by compressing the homogeneous powder mixture for five minutes under a pressure of 10 tons per square inch using a hydraulic press. Finally, the pellet was placed in the spectrometer for spectrum analysis. The spectra were collected as the average of 64 scans acquired in the spectral range from 1000 to 4000 cm^{-1} for FTIR analysis at room temperature.

DFT calculation was conducted to confirm the vibration of the hetero-molecular network. The electronic structure was calculated using the Density Functional Theory technique using the Gaussian16 package, Becke, 3-parameter, Lee-Yang-Parr (B3LYP) functional at the ground state with the 6-31G' basis set for the mixtures and individual components, respectively. The optimizations were performed using the Berny optimization algorithm in internal coordinates, with convergence acceleration via the default GDIIS (Geometry Direct Inversion in the Iterative Subspace) method. The maxi-mum number of SCF cycles was set to 128.

Amorphicity Determination

The degree of amorphicity in the samples was evaluated using X-ray diffraction (XRD) analysis. XRD patterns were obtained using a Rigaku Smartlab X-Ray Diffractometer equipped with a Cu Kα radiation (λ = 1.5406 Å) source. The samples were scanned over a 2θ range of 5°– 50° and a scan rate of 3°/min.

Results and Discussion

FTIR Analysis and DFT Calculation

Samples of ascorbic acid (AA), PVP K30 and their mixture were prepared and characterised using Fourier Transform Infrared (FTIR) Spectroscopy and calculated using DFT B3LYP/6-31G' basis set. These were used as references in the analysis by comparing them with the mixture, to validate and understand the molecular interactions and functional groups present in binary co-amorphous system (BCAS). The infrared bands observed for pure AA (x=100 mol%) [17-19] and PVP K30 (x=0 mol%) [15,20-22] were consistent with the data previously reported in the literature allowing for a thorough analysis of the molecular vibrations in the binary co-amorphous system (BCAS).

Altering the molecular environment, such as shifting from a crystalline to an amorphous state leads to frequency shifts and peak broadening, confirming the successful modification of the environment.[23] In the context of vibrational analysis, hydrogen bonding can cause shifts in the vibrational frequencies of the functional groups involved in bonding.[6,24-25] This phenomenon has been previously documented, with studies attributing the broadening of infrared frequencies to changes in crystal structure caused by molecular disorder, indicating an amorphous state.[23,26,27-28]

The infrared spectra, in the 3500–3200 cm^{-1} range, corresponding to the O-H group stretching vibration characteristic of the alcohol group in ascorbic acid (AA), exhibited notable broadening, especially in the x=60 sample. This broadening suggests the presence of extensive hydrogen bonding.[24] Notably, the C=O signal (originating from PVP) and the O-H signal (originating from AA) in the x=60 mol% mixture exhibits the lowest peak intensities compared to other mixtures and their pure individual components. The C=O stretching vibration of amorphous PVP shifts slightly from 1644.22 cm^{-1} (pure amorphous PVP) to 1644.19 cm^{-1} in the x=60 mol% sample, while the O-H peak of AA shifts from 1314.42 cm^{-1} to 1316.56 cm^{-1} in the same sample. For the C=O signal, initially observed at 1753.17 cm^{-1} in the crystalline state of ascorbic acid, shifts slightly to 1754.12 cm^{-1} [29] and shows a significant reduction in peak intensity, possibly due to intermolecular interactions with the CH_2 (ethyl groups) of PVP in the range of 2800-3600 cm^{-1}. These spectral changes are consistent with previous findings demonstrating that PVP K30 induces amorphization through intermolecular O–H···O=C hydrogen bonds, as evidenced by broadened OH stretching (around 3404 cm^{-1}) and CH stretching (around 3264 cm^{-1}) signals in myricetin, indicating PVP's ability to engage in such interactions.[25]

The red dotted lines represent simulated spectra generated by mathematically adding the individual FTIR spectra of pure AA and PVP K30 at specific weight ratios, assuming no molecular interactions. Comparing these to the experimental spectra (black lines) reveals spectral shifts, broadening, or intensity changes, indicating intermolecular interactions, particularly hydrogen bonding between AA and PVP. Notable deviations at certain compositions (x=60 mol%) suggest interactions. These spectral changes support the formation of co-amorphous systems with improved miscibility and physical stability.

These shifts, along with the observed broadening and reduced intensities in Figure 1., reflect hydrogen bonding that led to structural changes and contribute to the formation of an amorphous state within drug-polymer matrix.[26-27] These conclusions are further supported by X-ray diffraction (XRD) spectra (Figure 3.), which confirm a loss of hydrogen bonding interactions due to increased molecular disorder. The shift in the C=O stretching vibration of PVP K30 and AA suggests hydrogen bonding interactions between the hydroxyl groups of AA and ethyl group of PVP, respectively, as illustrated in Figure 3. These interactions play a role for AA to be dispersed into the PVP matrix, potentially promoting the formation of an amorphous state. Hydrogen bonding typically depends on concentration levels [28], as observed in the BCAS samples with x=60 mol%, which exhibit different results compared to other ratios. Moreover, the peak associated with AA molecules remain intact in the infrared spectra of samples with x=20,40 and 80 mol%.

Figure 1. illustrates the theoretical data (blue) calculated using DFT with the B3LYP/6-31G' basis set. At approximately 1442.27 cm^{-1} (CH), 1749.38 cm^{-1} (C=O), 1674.22 cm^{-1} (C=O), 3132.11 cm^{-1} (C-H) and 3510.04 cm^{-1} (O-H) indicates hydrogen bonding within the AA-PVP complex, as derived from theoretical calculations. In this work, the BCAS exhibited up to 168 normal modes, while the individual components demonstrated 54 modes for AA [29-30] and 51 modes for PVP [29], respectively which align with prior studies.

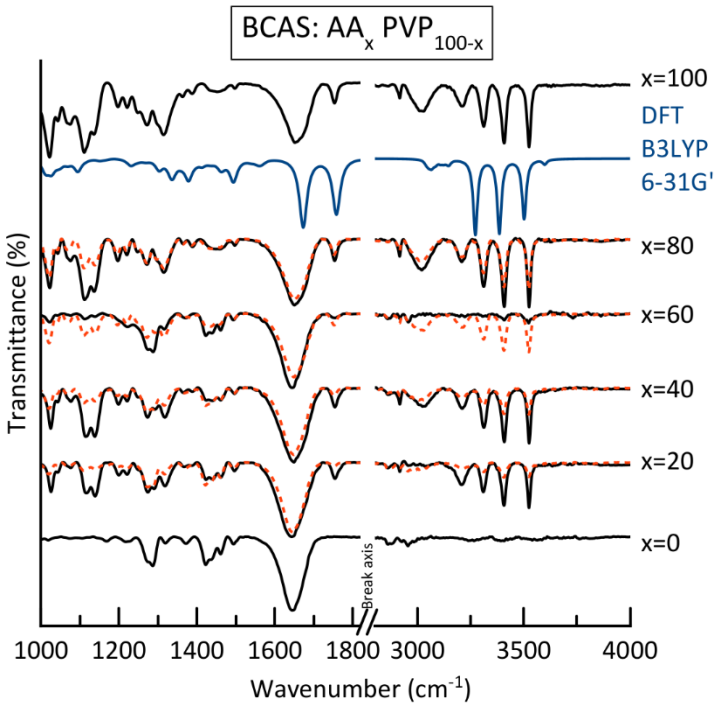

Figure 1. Normalized and corrected Infrared spectra of ascorbic acid, PVP K30, and the BCAS at varying compositions (mol%) with DFT calculations (B3LYP 6-31G'). The red dotted line represents the simulated pattern of the mixture

The structural properties of AA and PVP K30, revealed through their HOMO and LUMO distributions, highlight their distinct reactivities, as shown in Figure 2. For AA, the HOMO and LUMO were delocalized around the lactone ring.[30] This delocalization suggests a high electron density, making ascorbic acid an effective electron donor.[31] In contrast, for PVP K30, the HOMO was delocalized around the C=O group in the pyrrolidone ring and the ethyl group, identifying regions prone to electron donation. Meanwhile, the LUMO was localized around the carbonyl group of the pyrrolidone ring, indicating regions likely to participate in electron acceptance. In a prior study, the HOMO of PVP K30 was found on the oxygen atom of the C=O group, suggesting potential sites for nucleophilic activity, while the LUMO was distributed across the molecule, excluding the C=O site.[29] The interaction of molecules in the mixture was determined by considering the nature of the reacting molecules of individual components. The binding energy of isolated and interacting molecules of PVP K30 and AA shows that the HOMO-LUMO energy gap, $E_{HOMO-LUMO}$, is higher for isolated molecules than for interacting ones (Table 1). The reduction of the energy band gap for interacting molecules shows a formation of new electronic states due to orbital hybridization between the two materials. When multiple materials come together in one system, their atomic orbitals with similar energy levels can slightly overlap.[32]

The calculated energy gap for PVP K30 (-0.25968 eV) is higher than that of ascorbic acid (-0.18419 eV) due to its structural and stability properties. When PVP K30 was added to AA, its decrease the energy bandgap of the AA in the mixture. In a co-amorphous system, the overlap of molecular orbitals between different components can enhance electronic delocalization, effectively lowering the energy required for an electron to transition from the HOMO to the LUMO.[33] The reduction in the HOMO–LUMO energy gap of the mixture generally indicates greater reactivity indicating successful forming an amorphous state.[29] This might contribute to the physicochemical properties of the co-amorphous system.[34] Next, the dipole moment values for interacting molecules were higher than the individual isolated molecule indicating strong polarity. Strong polarity contributes to its ability to form hydrogen bonding and significantly impacts the physical properties of substances.[34] An increased dipole moment for interacting molecules shows that the presence of hydrogen bonding enhances the overall dipole moment of the system.[33,35-36] Following, PVP K30 molecule has the highest chemical hardness and has the least tendency to react as it has been recorded to be the most stable molecule with the least reactivity compared to ascorbic acid (AA) and its interacting molecules.[37] Furthermore, the decrease in the electronegativity in the interacting molecules indicate a lower tendency to attract electrons, as part of their electron density is delocalized or shifted toward the interaction sites [38].

Table 1. Electronic properties for isolated and interacting molecules

Molecule name	Equations	AA	PVP K30	BCAS
Basis Set		6-31G'	6-31G'	6-31G'
E_{HOMO} (eV)		-0.22843	-0.23174	-0.19002
E_{LUMO} (eV)		-0.04424	0.02794	-0.01878
$E_{HOMO-LUMO}$ (eV)		-0.18419	-0.25968	-0.17124
Chemical hardness, η (eV)	$\eta = (E_{LUMO} - E_{HOMO})/2$	0.092095	0.12984	0.08562
Chemical potential, μ (eV)	$\mu = (E_{HOMO} + E_{LUMO})/2$	-0.136335	-0.1019	-0.1044
Electronegativity, χ (eV)	$\chi = -(E_{HOMO} + E_{LUMO})/2$	0.136335	0.1019	0.1044
Electrophilicity index	$\omega = \mu^2/2\eta$	-0.100913	0.03999	0.06365
Dipole moment (debye)		4.7195584	4.1550342	13.16979

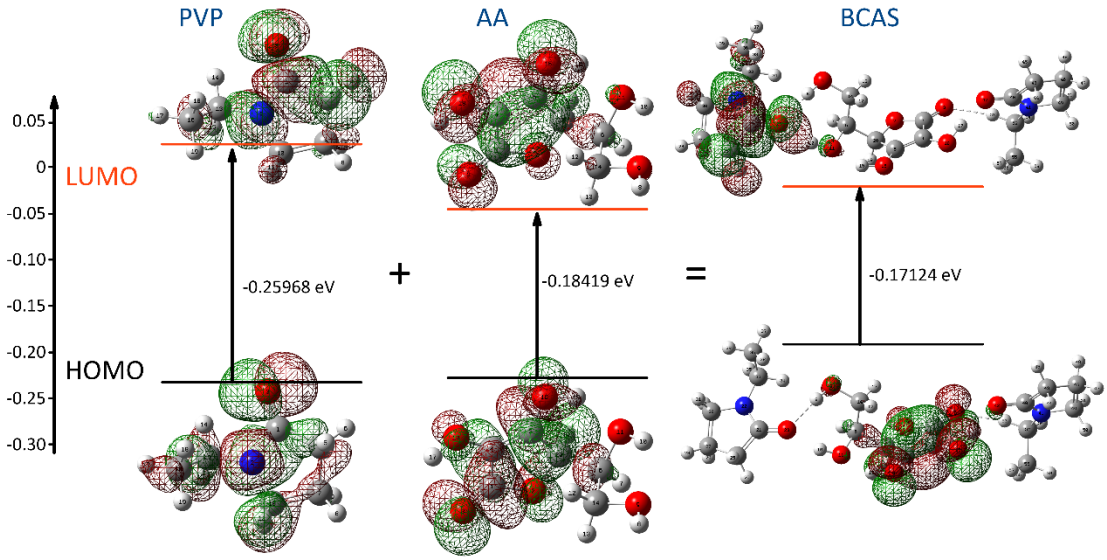

Figure 2. Optimized molecular structure, HOMO and LUMO orbital levels and energy gap of AA, PVP K30 and BCAS calculated with DFT at the B3LYP/6-31G' level using Gaussian16 package. HOMO and LUMO represent the frontier orbitals indicating electron donation (HOMO) and acceptance (LUMO) sites

Figure 3. displays the molecular electrostatic potential (MEP) serves as a predictor of chemical reactivity. The red colour with negative indicates the minimum electrostatic potential (that means it is bound loosely or has excess electrons) and acts as an electrophilic attack. The blue indicates the maximum electrostatic potential, and it acts as nucleophilic. The MEP reveals the partial distribution of charge along the molecule's surface to provide insights into the electrostatic nature of the molecule, which is essential for drug interactions.[29,36] It reflects the molecule's dipole moments, electronegativity, partial charges, and chemical reactivity, indicating the net electrostatic effect produced at a point in the space around the molecule by its total charge distribution (electrons and nuclei).

The MEP of individual component reveals that oxygen atoms in the carbonyl (C=O) groups of PVP K30 and the phenol group (OH) of ascorbic acid (AA) exhibit high electron densities. The MEP surface of the AA-PVP complex provides clear evidence of electron transfer between molecules resulting in a changed in electron density around the interaction sites. High electron density (negative potential) is observed in the phenol ring of AA, which contains abundant O-H groups and gains additional electrons from the C=O bond of PVP K30 in the mixture. In contrast, low electron density (positive to almost zero potential) around PVP K30 highlights its role in stabilizing the structure through hydrogen bonding. PVP primarily facilitates electron transfer by donating electrons through its C=O bond to AA, balancing the system's overall electrostatic potential. These findings are supported by observed increases and decreases in electrostatic potential at the bonding sites on the MEP surface.

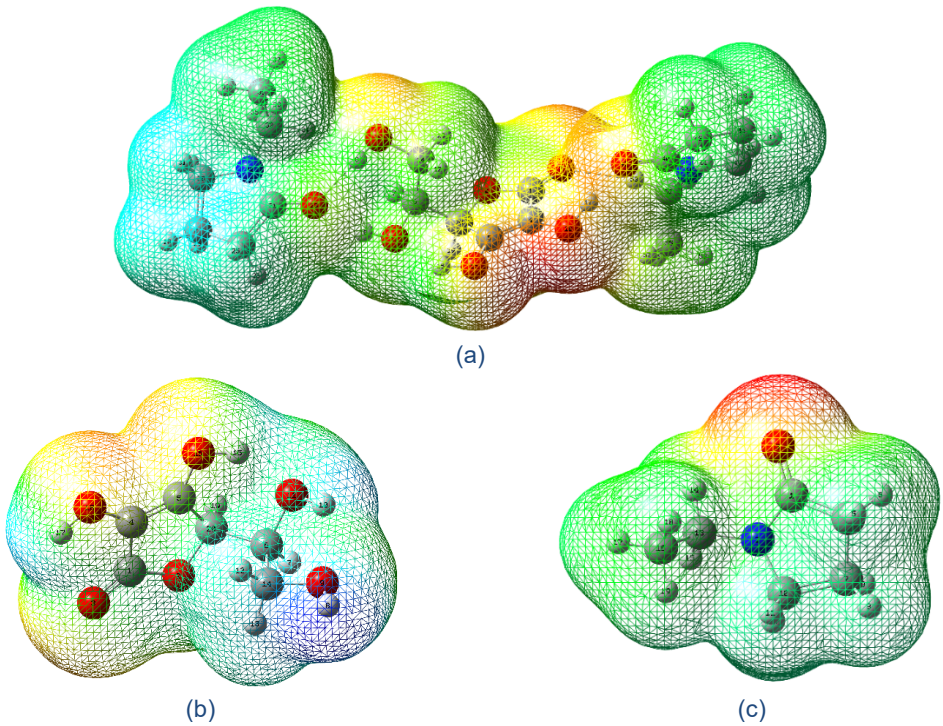

Figure 3. Molecular Electrostatic Potential (MEP) of (a) the BCAS, (b) Ascorbic acid and (c) PVP K30. The molecular surface displays varying colours: red for negative, blue for positive, and green for neutral electrostatic potentials

Figure 4. presents the XRD patterns of AA_xPVP_{100-x} samples with varying molar ratios (x = 0–100 mol%). The diffractogram of pure AA (x = 100 mol%) shows sharp and intense peaks characteristic of a highly crystalline structure. As the PVP content increases (x = 80 to 60 mol%), peak intensities begin to decrease, accompanied by slight broadening, indicating a partial reduction in crystallinity. At x = 40 mol%, a further reduction in intensity, while the x = 20 mol% sample shows a broad halo with residual crystalline peaks, suggesting a significant amorphous contribution. In contrast, the x = 0 mol% sample (pure PVP K30) exhibits a broad halo, confirming its fully amorphous nature.

These XRD observations indicate that PVP K30 promotes partial amorphization of AA, though full reduction of crystallinity is not achieved at higher AA contents. This limitation is likely due to AA's inherent crystallinity as a GFA Class I compound, which tends to recrystallize rapidly and shows limited miscibility with polymers.[1] Amorphization only occurred when AA content was slightly reduced (x ≤ 20 mol%), allowing PVP to more effectively inhibit recrystallization. Notably, recent studies have demonstrated the formation of amorphous ascorbic acid when lyophilized with polymers PVP at 50% [1] and ≤70% (w/w) AA:PVP ratios [2], highlighting the influence of preparation method and component ratio.

The broadening of IR peaks (x=60 mol%) reflects various hydrogen bonding interactions between AA and PVP K30, indicating localized disruptions in the molecular arrangement without fully disrupting the crystalline lattice. This can be explained by the fact that XRD detects long-range crystalline order, while infrared spectroscopy is more sensitive to local changes and molecular interactions [39]. This observation aligns with a previous study on the dispersion of Lacidipine with PVP K30, which reported both broad and sharp peaks in its XRD spectra, likely due to the hygroscopic nature of PVP K30.[16] The use of melt-quenching, which may be less effective than lyophilization in disrupting the crystalline network of AA, as a 1:1 AA-PVP ratio was successfully formed in an amorphous state via lyophilization in a prior study.[1-2] Additionally, other studies on drug dissolution have shown that using modified solvent methods can also lead to successful amorphization, offering another potential route for preparing co-amorphous systems.[13,26] This discrepancy could be attributed to differences in preparation methods, as lyophilization and solvent evaporation used in previous studies may more effectively prevent recrystallization compared to the melt-quench method employed here.

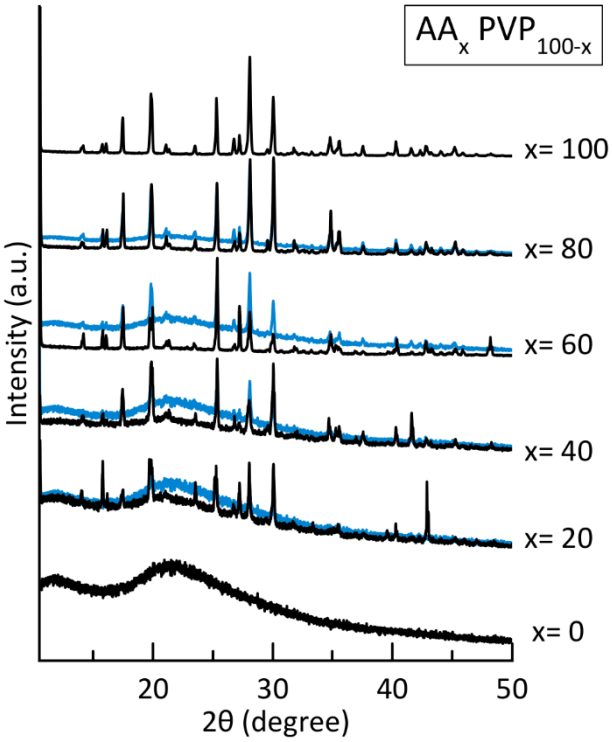

Figure 4. Normalized XRD diffractogram of AA:PVP K30 mixtures at varying compositions (x = 0–100 mol%). The blue line represents the simulated pattern of the mixture

Conclusions

This study investigated the molecular structures of samples with varying compositions by analysing their FTIR vibrational spectra to identify intermolecular interaction linked to compositional changes. As vibrational data offer only qualitative insights into molecular units, computational analysis using Gaussian16 was employed to interpret the spectra, predict molecular properties, and enhance structural understanding.

This study elucidates the structural and molecular interactions for ascorbic acid (AA) in a co-amorphous system with PVP K30. The FTIR spectra indicate significant hydrogen bonding interactions, leading to peak broadening and shifts, which are further supported by DFT calculations showing reduced HOMO-LUMO energy gaps and increased dipole moments. XRD results reveal a reduction in crystallinity (broadening of peaks), indicating partial amorphization across the compositions, with residual semi-crystalline features still present at lower AA content. The findings demonstrate that PVP K30 does interact with AA at molecular level. However, despite these improvements, the study also reveals that complete amorphization is not fully achieved, likely due to the inherent hygroscopic nature of PVP K30 or the limitations of the melt-quenching technique. Additionally, future research should explore alternative polymer ratios, preparation methods, or additional stabilizing agents to further enhance the long-term stability of co-amorphous AA formulations.

Conflicts of Interest

The author(s) declare(s) that there is no conflict of interest regarding the publication of this paper.

Acknowledgment

We thanks to Ministry of Higher Education (MOHE) for providing funding support for this Fundamental Research Grant Scheme project FRGS/1/2023/STG07/UNISZA/022, and UTM through Q.J130000.21A2.05E65.

References

[1] Christina, B., Taylor, L. S., & Mauer, L. J. (2015). Physical stability of L-ascorbic acid amorphous solid dispersions in different polymers: A study of polymer crystallization inhibitor properties. *Food Research International, 76*, 867–877.

[2] Sanchez, J. O., Ismail, Y., Christina, B., & Mauer, L. J. (2018). Degradation of L-ascorbic acid in the amorphous solid state. *Journal of Food Science, 83*(3), 670–681.

[3] Nayak, G., Trivedi, M., Branton, A., Trivedi, D., & Jana, S. (2019). Physicochemical and thermal characterization of ascorbic acid: Impact of biofield energy treatment. *Journal of Pharmaceutical and Pharmacological Sciences, 1*(2019).

[4] Yin, X., Chen, K., Cheng, H., Chen, X., Feng, S., Song, Y., & Liang, L. (2022). Chemical stability of ascorbic acid integrated into commercial products: A review on bioactivity and delivery technology. *Antioxidants, 11*(1), 153.

[5] Mehmood, T., Ahmed, A., Ahmad, Z., Javed, M. S., Sharif, H. R., Shah, F. U. H., ... & Murtaza, S. (2022). Physicochemical characteristics of mixed surfactant-stabilized L-ascorbic acid nanoemulsions during storage. *Langmuir, 38*(31), 9500–9506.

[6] Kilpeläinen, T., Ervasti, T., Uurasjärvi, E., Koistinen, A., Ketolainen, J., Korhonen, O., & Pajula, K. (2022). Detecting different amorphous–amorphous phase separation patterns in co-amorphous mixtures with high resolution imaging FTIR spectroscopy. *European Journal of Pharmaceutics and Biopharmaceutics, 180*, 161–169.

[7] Rautaniemi, K., Vuorimaa-Laukkanen, E., Strachan, C. J., & Laaksonen, T. (2018). Crystallization kinetics of an amorphous pharmaceutical compound using fluorescence-lifetime-imaging microscopy. *Molecular Pharmaceutics, 15*(5), 1964–1971.

[8] Ismail, Y., & Mauer, L. J. (2020). Phase transitions of ascorbic acid and sodium ascorbate in a polymer matrix and effects on vitamin degradation. *Journal of Food Process Engineering, 43*(5), e13073.

[9] Park, H., Seo, H. J., Hong, S. H., Ha, E. S., Lee, S., Kim, J. S., ... & Hwang, S. J. (2020). Characterization and therapeutic efficacy evaluation of glimepiride and L-arginine co-amorphous formulation prepared by supercritical antisolvent process: Influence of molar ratio and preparation methods. *International Journal of Pharmaceutics, 581*, 119232.

[10] Wdowiak, K., Tajber, L., Miklaszewski, A., & Cielecka-Piontek, J. (2024). Sweeteners show a plasticizing effect on PVP K30—A solution for the hot-melt extrusion of fixed-dose amorphous curcumin-hesperetin solid dispersions. *Pharmaceutics, 16*(5), 659.

[11] Saberi, A., Kouhjani, M., Yari, D., Jahani, A., Asare-Addo, K., Kamali, H., & Nokhodchi, A. (2023). Development, recent advances, and updates in binary, ternary co-amorphous systems, and ternary solid dispersions. *Journal of Drug Delivery Science and Technology*, 104746.

[12] Bejaoui, M., Galai, H., Amara, A. B. H., & Ben Rhaiem, H. (2019). Formation of water soluble and stable amorphous ternary system: Ibuprofen/β-cyclodextrin/PVP. *Glass Physics and Chemistry, 45*, 580–588.

[13] Malkawi, R., Malkawi, W. I., Al-Mahmoud, Y., & Tawalbeh, J. (2022). Current trends on solid dispersions: Past, present, and future. *Advances in Pharmacological and Pharmaceutical Sciences, 2022*(1), 5916013.

[14] Riekes, M. K., Engelen, A., Appeltans, B., Rombaut, P., Stulzer, H. K., & Van den Mooter, G. (2016). New perspectives for fixed dose combinations of poorly water-soluble compounds: A case study with ezetimibe and lovastatin. *Pharmaceutical Research, 33*, 1259–1275

[15] Orszulak, L., Lamrani, T., Tarnacka, M., Hachuła, B., Jurkiewicz, K., Zioła, P., ... & Kamiński, K. (2024). The impact of various poly(vinylpyrrolidone) polymers on the crystallization process of metronidazole. *Pharmaceutics, 16*(1), 136.

[16] Sun, M., Wu, C., Fu, Q., Di, D., Kuang, X., Wang, C., ... & Sun, J. (2016). Solvent-shift strategy to identify suitable polymers to inhibit humidity-induced solid-state crystallization of lacidipine amorphous solid dispersions. *International Journal of Pharmaceutics, 503*(1–2), 238–246.

[17] Zapata, F., López-Fernández, A., Ortega-Ojeda, F., Quintanilla, G., García-Ruiz, C., & Montalvo, G. (2021). Introducing ATR-FTIR spectroscopy through analysis of acetaminophen drugs: Practical lessons for interdisciplinary and progressive learning for undergraduate students. *Journal of Chemical Education, 98*(8), 2675–2686.

[18] Singh, G., Mohanty, B. P., & Saini, G. S. S. (2016). Structure, spectra and antioxidant action of ascorbic acid studied by density functional theory, Raman spectroscopic and nuclear magnetic resonance techniques. *Spectrochimica Acta Part A: Molecular and Biomolecular Spectroscopy, 155*, 61–74.

[19] Barra, P. A., Márquez, K., Gil-Castell, O., Mujica, J., Ribes-Greus, A., & Faccini, M. (2019). Spray-drying performance and thermal stability of L-ascorbic acid microencapsulated with sodium alginate and gum Arabic. Molecules, 24(16), 2872.

[20] Orszulak, L., Lamrani, T., Bernat, R., Tarnacka, M., Żakowiecki, D., Jurkiewicz, K., ... & Kamińska, E. (2024). The influence of PVP polymer topology on the liquid crystalline order of itraconazole in binary systems. *Molecular Pharmaceutics.*

[21] Joseph, A., & Mathew, S. (2021). Electronic properties of PVP-ionic liquid composite: Spectroscopic and DFT-based thermochemical studies on the effect of anions. *Iranian Polymer Journal, 30*(5), 505–512.

[22] Blinov, A. V., Nagdalian, A. A., Povetkin, S. N., Gvozdenko, A. A., Verevkina, M. N., Rzhepakovsky, I. V., ... & Shariati, M. A. (2022). Surface-oxidized polymer-stabilized silver nanoparticles as a covering component of suture materials. *Micromachines, 13*(7), 1105.

[23] Guinet, Y., Paccou, L., & Hédoux, A. (2023). Mechanism for stabilizing an amorphous drug using amino acids within co-amorphous blends. *Pharmaceutics, 15*(2), 337.

[24] Zeinalipour-Yazdi, C. D., & Loizidou, E. Z. (2021). An experimental FTIR-ATR and computational study of H-bonding in ethanol/water mixtures. *Chemical Physics, 550*, 111295.

[25] Rosiak, N., Tykarska, E., & Cielecka-Piontek, J. (2024). Myricetin amorphous solid dispersions—

Antineurodegenerative potential. *Molecules, 29*(6), 1287.
[26] Chavan, R. B., Lodagekar, A., Yadav, B., & Shastri, N. R. (2020). Amorphous solid dispersion of nisoldipine by solvent evaporation technique: Preparation, characterization, in vitro, in vivo evaluation, and scale-up feasibility study. *Drug Delivery and Translational Research, 10*, 903–918.
[27] Browne, E., Worku, Z. A., & Healy, A. M. (2020). Physicochemical properties of poly-vinyl polymers and their influence on ketoprofen amorphous solid dispersion performance: A polymer selection case study. *Pharmaceutics, 12*(5), 433.
[28] Martínez, L. M., Videa, M., Sosa, N. G., Ramírez, J. H., & Castro, S. (2016). Long-term stability of new co-amorphous drug binary systems: Study of glass transitions as a function of composition and shelf time. *Molecules, 21*(12), 1712.
[29] Refaat, A., & Ibrahim, M. (2024). Microspectroscopic, DFT and QSAR study of PVP/$CaCO_3$ blends as potential bone-remineralization membranes. *Egyptian Journal of Chemistry, 67*(2), 29–41.
[30] Nasidi, I. I., Kaygili, O., Majid, A., Bulut, N., Alkhedher, M., & ElDin, S. M. (2022). Halogen doping to control the band gap of ascorbic acid: A theoretical study. *ACS Omega, 7*(48), 44390–44397.
[31] Ahmed, L., & Omer, R. (2020). Spectroscopic properties of vitamin C: A theoretical work. *Cumhuriyet Science Journal, 41*(4), 916–928.
[32] Scharber, M. C., & Sariciftci, N. S. (2021). Low band gap conjugated semiconducting polymers. *Advanced Materials Technologies, 6*(4), 2000857.
[33] Choudhary, V., Bhatt, A., Dash, D., & Sharma, N. (2019). DFT calculations on molecular structures, HOMO–LUMO study, reactivity descriptors and spectral analyses of newly synthesized diorganotin (IV) 2-chloridophenylacetohydroxamate complexes. *Journal of Computational Chemistry, 40*(27), 2354–2363.
[34] Adekoya, O. C., Adekoya, G. J., Sadiku, E. R., Hamam, Y., & Ray, S. S. (2022). Application of DFT calculations in designing polymer-based drug delivery systems: An overview. *Pharmaceutics, 14*(9), 1972.
[35] Tchouadji Ndjike, M. B., Tchakoutio Nguetcho, A. S., Li, J., & Bilbault, J. M. (2021). Interplay role between dipole interactions and hydrogen bonding on proton transfer dynamics. *Nonlinear Dynamics, 105*(3), 2619–2643.
[36] Kazemi, S., Daryani, A. S., Abdouss, M., & Shariatinia, Z. (2016). DFT computations on the hydrogen bonding interactions between methacrylic acid-trimethylolpropane trimethacrylate copolymers and letrozole as drug delivery systems. *Journal of Theoretical and Computational Chemistry, 15*(02), 1650015.
[37] El Kassimi, A., Boutouil, A., El Himri, M., Laamari, M. R., & El Haddad, M. (2020). Selective and competitive removal of three basic dyes from single, binary and ternary systems in aqueous solutions: A combined experimental and theoretical study. *Journal of Saudi Chemical Society, 24*(7), 527–544.
[38] Zhou, Y., Hao, W., Zhao, X., Zhou, J., Yu, H., Lin, B., ... & Fan, H. J. (2022). Electronegativity-induced charge balancing to boost stability and activity of amorphous electrocatalysts. *Advanced Materials, 34*(11), 2100537.
[39] Guerrero-Pérez, M. O., & Patience, G. S. (2020). Experimental methods in chemical engineering: Fourier transform infrared spectroscopy—FTIR. *The Canadian Journal of Chemical Engineering, 98*(1), 25–33.